Mineralogical Magazine, October 2012, Vol. 76(5), pp. 1133–1152

The sulfite anion in ettringite-group minerals: a new mineral species hielscherite, $Ca_3Si(OH)_6(SO_4)(SO_3)\cdot 11H_2O$, and the thaumasite–hielscherite solid-solution series

I. V. Pekov[1,*], N. V. Chukanov[2], S. N. Britvin[3], Y. K. Kabalov[1], J. Göttlicher[4], V. O. Yapaskurt[1], A. E. Zadov[5], S. V. Krivovichev[3], W. Schüller[6] and B. Ternes[7]

[1] Faculty of Geology, Moscow State University, Vorobievy Gory, 119991 Moscow, Russia
[2] Institute of Problems of Chemical Physics, Russian Academy of Sciences, Chernogolovka, 142432 Moscow, Russia
[3] Faculty of Geology, St Petersburg State University, Universitetskaya Nab. 7/9, St. Petersburg, 199034 Russia, and Nanomaterials Research Centre, Kola Science Center RAS, Fersman Str. 20, 184200 Apatity, Russia
[4] Karlsruhe Institute of Technology, Institute for Synchrotron Radiation, Hermann von Helmholtz Platz 1, D-76344 Eggenstein-Leopoldshafen, Germany
[5] NPP "Teplokhim", Dmitrovskoye Avenue 71, 127238 Moscow, Russia
[6] Im Strauβenpesch 22, 53518 Adenau, Germany
[7] Bahnhofstrasse 45, 56727 Mayen, Germany

[*Received 22 April 2012; Accepted 16 July 2012; Associate Editor: Stuart Mills*]

ABSTRACT

Hielscherite, ideally $Ca_3Si(OH)_6(SO_4)(SO_3)\cdot 11H_2O$, (IMA 2011-037) is the first ettringite-group mineral with essential sulfite. We have identified a continuous natural solid-solution series from endmember thaumasite, $Ca_3Si(OH)_6(SO_4)(CO_3)\cdot 12H_2O$, to a composition with at least 77 mol.% endmember hielscherite. In this series, the SO_3:CO_3 ratio is variable, whereas the SO_4 content remains constant. Compositions with more than 50 mol.% endmember hielscherite have only been found at Graulay quarry near Hillesheim in the western Eifel Mountains, Rhineland-Palatinate, where they occur with phillipsite-K, chabazite-Ca and gypsum in cavities in alkaline basalt. Sulfite-rich thaumasite has been found in hydrothermal assemblages in young alkaline basalts in two volcanic regions of Germany: it is widespread at Graulay quarry and occurs at Rother Kopf, Schellkopf and Bellerberg quarries in Eifel district; it has also been found at Zeilberg quarry, Franconia, Bavaria. Hielscherite forms matted fibrous aggregates up to 1 cm across and groups of acicular to prismatic hexagonal crystals up to $0.3 \times 0.3 \times 1.5$ mm. Individual crystals are colourless and transparent with a vitreous lustre and crystal aggregates are white with a silky lustre. The Mohs hardness is 2–2½. Measured and calculated densities are D_{meas} = 1.82(3) and D_{calc} = 1.79 g cm^{-3}. Hielscherite is optically uniaxial (–), ω = 1.494(2), ε = 1.476(2). The mean chemical composition of holotype material (determined by electron microprobe for Ca, Al, Si, and S and gas chromatography for C, H and N, with the S^{4+}:S^{6+} ratio from the crystal-structure data) is CaO 27.15, Al_2O_3 2.33, SiO_2 7.04, CO_2 2.71, SO_2 6.40, SO_3 12.91, N_2O_5 0.42, H_2O 39.22, total 98.18 wt.%. The empirical formula on the basis of 3 Ca atoms per formula unit is $Ca_3(Si_{0.73}Al_{0.28})_{\Sigma 1.01}(OH)_{5.71}(SO_4)_{1.00}(SO_3)_{0.62}(CO_3)_{0.38}(NO_3)_{0.05}\cdot 10.63H_2O$. The presence of sulfite was confirmed by crystal-structure analysis and infrared and X-ray absorption near

* E-mail: igorpekov@mail.ru
DOI: 10.1180/minmag.2012.076.5.06

edge structure spectra. The crystal structure of sulfite-rich thaumasite from Zeilberg quarry was solved by direct methods based on single-crystal X-ray diffraction data (R_1 = 0.064). The structure of hielscherite was refined using the Rietveld method (R_{wp} = 0.0317). Hielscherite is hexagonal, $P6_3$, a = 11.1178(2), c = 10.5381(2) Å, V = 1128.06(4) Å^3 and Z = 2. The strongest reflections in the X-ray powder pattern [(d,Å)(I)(hkl)] are: 9.62(100)(010,100); 5.551(50)(110); 4.616(37)(012,102); 3.823(64)(112); 3.436(25)(211), 2.742(38)(032,302), 2.528(37)(123,213), 2.180(35)(042,402;223). In both hielscherite and sulfite-rich thaumasite, pyramidal sulfite groups occupy the same site as trigonal carbonate groups, with analogous O sites, whereas tetrahedral sulfate groups occupy separate positions. Hielscherite is named in honour of the German mineral collector Klaus Hielscher (b. 1957).

Keywords: hielscherite, new mineral, thaumasite, ettringite group, sulfite, crystal structure, IR spectroscopy, XANES spectroscopy, alkaline basalt, cement, concrete, Eifel, Graulay, Zeilberg.

Introduction

THE ettringite group is made up of highly hydrated hexagonal or trigonal basic salts with a general formula $Ca_6M_2(OH)_{12}R_{3-4}{\cdot}nH_2O$, where M = Al^{3+}, Cr^{3+}, Fe^{3+}, Si^{4+}, Mn^{4+} or Ge^{4+} are species-defining cations and R = SO_4^{2-}, CO_3^{2-}, SO_3^{2-}, PO_3OH^{2-} or $B(OH)_4^-$ are species-defining anions (Table 1). Eleven ettringite-type compounds have been described as mineral species and numerous synthetic compositions are known. Their structures are based on infinite $Ca_3[M(OH)_6(H_2O)_m]$ columns of $M(OH)_6$ octahedra, and trimers of edge-sharing Ca-centred polyhedra $Ca(OH)_4(H_2O)_x$ (the value of x and the corresponding coordination of Ca depend on the number of H_2O molecules in the mineral formula; Skoblinskaya *et al*., 1975). The R anions are located in channels that run parallel to the c axis. Ettringite-group minerals with $M = Si^{4+}$ contain Si atoms in octahedral coordination, which is extremely rare in nature (Jacobsen *et al*., 2003).

Sulfate is the most common species-defining anion in ettringite-group minerals (Table 1). Thaumasite, $Ca_3Si(OH)_6(SO_4)(CO_3){\cdot}12H_2O$, is the only widespread member of the group. Sulfite has not been reported in ettringite-group minerals to date, although the synthetic sulfite analogue of ettringite is well known (Pöllmann *et al*., 1989; Motzet and Pöllmann, 1999; Grier *et al*., 2002). Synthetic analogues of ettringite-group minerals are common constituents of cement and concrete (Batic *et al*., 2000; Brown and Hooton, 2002; Brown *et al*., 2003).

In this paper we describe hielscherite, an analogue of thaumasite with sulfite as a species-defining anion. Members of the thaumasite–hielscherite series have been identified in hydrothermal assemblages in young alkaline basalts in two volcanic regions of Germany, the Eifel (Rhineland-Palatinate) and Franconia (Bavaria). The presence of sulfite groups in these minerals was detected by infrared (IR) spectroscopy and confirmed by independent techniques including X-ray absorption near edge structure (XANES) spectroscopy and crystal structure analysis.

The new mineral hielscherite (Cyrillic: хильшерит) was named in honour of the German mineral collector Klaus Hielscher (b. 1957) from Steinbach, Hessen, a specialist in the mineralogy of hydrothermal assemblages from the Zeilberg basalt quarry in Franconia, a locality which is remarkable for its diverse hydrous calcium silicate minerals (Weiss, 1990). Sulfite-bearing thaumasite was first identified on a sample collected by K. Hielscher at Zeilberg quarry and this prompted us to look for other sulfite-bearing ettringites.

The new mineral and its name have been approved by the IMA Commission on New Minerals, Nomenclature and Classification (IMA 2011−037). The type specimen of hielscherite is deposited in the collections of the Fersman Mineralogical Museum of the Russian Academy of Sciences, Moscow, registration number 4093/1.

Hielscherite, $Ca_3Si(OH)_6(SO_4)(SO_3){\cdot}11H_2O$, is the fifth mineral which has sulfite as a species-defining anion, the others are scotlandite, $PbSO_3$ (Paar *et al*., 1984); hannebachite, $CaSO_3{\cdot}0.5H_2O$ (Hentschel *et al*., 1985); gravegliaite, $MnSO_3{\cdot}3H_2O$ (Basso *et al*., 1991); and orschallite, $Ca_3(SO_4)(SO_3)_2{\cdot}12H_2O$ (Weidenthaler *et al*., 1993).

Occurrence and appearance

Hielscherite

Hielscherite is known only on specimens from the Graulay (other versions of spelling are Graulai, Grauley, or Graulei) basalt quarry, near Hillesheim, in the western Eifel Mountains,

TABLE 1. Comparative crystal data for ettringite-group minerals.

Mineral	Simplified formula*	Space group	a (Å); c (Å)	References
Ettringite	$Ca_3Al(OH)_6(SO_4)_{1.5}\cdot 13H_2O$	$P31c$	11.26; 21.48	Moore and Taylor (1970)
Charlesite	$Ca_3(Al,Si)(OH,O)_6(SO_4)[B(OH)_4]_{0.5}\cdot 13H_2O$	$P31c$?	11.16; 21.21	Dunn *et al.* (1983)
Micheelsenite	$Ca_3Al(OH)_6(PO_3OH,CO_3)(CO_3)\cdot 12H_2O$	$P6_3$	10.83; 10.52	McDonald *et al.* (2001)
Bentorite	$Ca_3(Cr,Al)(OH)_6(SO_4)_{1.5}\cdot 13H_2O$	$P6_3/mmc$?	11.06; 10.63	Gross (1980)
Sturmanite	$Ca_3(Fe^{3+},Al,Mn^{4+})(OH)_6(SO_4)_{1.5}[B(OH)_4]_{0.5}\cdot 12H_2O$	$P31c$	11.19; 21.91	Pushcharovsky *et al.* (2004)
Jouravskite	$Ca_3Mn^{4+}(OH)_6(SO_4,CO_3)_2\cdot 13H_2O$	$P6_3$	11.06; 10.50	Granger and Protas (1969)
Carraraite	$Ca_3Ge(OH)_6(SO_4,CO_3)_2\cdot 12H_2O$	$P6_3/m$	11.06; 10.63	Merlino and Orlandi (2001)
Buryatite	$Ca_3(Si,Fe^{3+},Al)(OH,O)_6(SO_4)[B(OH)_4]\cdot 12H_2O$	$P31c$?	11.14; 20.99	Malinko *et al.* (2001)
Thaumasite	$Ca_3Si(OH)_6(SO_4)(CO_3)\cdot 12H_2O$	$P6_3$	11.02–11.08; 10.37–10.44	Effenberger *et al.* (1983); Anthony *et al.* (1995); Martucci and Cruciani (2006)
Kottenheimite	$Ca_3Si(OH)_6(SO_4)_2\cdot 12H_2O$	$P6_3/m$	11.15; 10.57	Chukanov *et al.* (2012)
Hielscherite	$Ca_3Si(OH)_6(SO_4)(SO_3)\cdot 11H_2O$	$P6_3$	11.12; 10.54	this study

* Calculated on the basis of 3 Ca atoms per formula unit.

Rhineland-Palatinate (Rheinland-Pfalz), Germany. The holotype specimen (described here using the code G-3049; no. 11 in Table 2) was found by one of the authors (IVP) in April 2010. In 2011 further specimens, which added information about the morphology and associations of the new mineral, were collected.

Hielscherite was first identified in miarolitic cavities up to 5 × 8 mm across, lined with early diopside and later phillipsite-K, on specimen G-3049. In this assemblage it occurs as acicular to hair-like crystals with an irregular polygonal cross section (Fig. 1), which are typically split (divergent) and/or curved. The crystals overgrow phillipsite-K and are rarely found as intergrowths with this zeolite (Fig. 2). The crystals on the holotype hielscherite specimen are typically 0.05 mm in length, rarely up to 0.2 mm long, and typically 3–5 μm thick. They occur in near parallel or sheaf-like clusters (Fig. 2) up to 10 μm thick, which form open chaotic fibrous aggregates up to 4 mm across, resembling matted wool (Fig. 3*a*).

Further fieldwork showed that hielscherite is most common in xenoliths of volcanic glass. It occurs in spherical cavities in fresh glass and in cavities and cracks in altered xenoliths with fine-grained aggregates of zeolites and clay minerals. In this assemblage, hielscherite has been identified in aggregates similar to those described on the holotype specimen, filling cavities up to 2 mm in diameter (Fig. 3*b*), and in cauliflower-like clusters up to 1 cm across (sample G-3229; no. 10 in Table 2). In some specimens, euhedral hexagonal prismatic crystals up to 1.5 mm long and 0.3 mm across, bounded by {100} and {001},

FIG. 1. Crystals of hielscherite on the holotype specimen (G-3049) from Graulay quarry. Secondary electron SEM image.

TABLE 2. Chemical composition of minerals of the thaumasite–hielscherite solid-solution series; only Ca, Al, Si and S contents obtained from electron microprobe data are given.

Number*	1	2	3	4	5	6	7	8	9	10	11**	12**	13
Code†	G-3226	R-3240	Zb-01	G-3238	G-3225	G-3235	S-3239	G-3230	G-3227	G-3229	G-3049	G-3231	G-3234
wt.%													
CaO	30.58	30.52	27.77	29.83	29.68	28.79	28.30	28.90	28.12	27.77	27.15	27.72	26.63
Al_2O_3	0.90	0.79	0.25	1.62	4.51	0.67	3.38	0.41	0.78	0.48	2.33	1.06	1.10
SiO_2	10.06	9.89	9.72	8.77	5.42	9.39	6.25	9.71	8.95	9.42	7.04	8.50	8.36
$SO_{2\ calc}$‡	0.23	0.93	2.12	2.44	2.88	3.40	3.82	4.40	4.59	5.76	6.40	6.96	7.80
$SO_{3\ calc}$‡	14.55	14.55	13.23	14.20	14.12	13.71	13.46	13.74	13.82	13.21	12.91	13.19	12.66
Total	56.32	56.68	53.09	56.86	56.71	55.96	55.21	57.16	56.26	56.64	55.83	57.43	56.55
$SO_{3\ meas}$	14.84	15.71	15.87	17.25	17.72	17.96	18.24	19.24	19.56	20.41	20.91	21.89	22.40
Formula calculated on the basis of 6 Ca atoms per formula unit (Z = 1)													
Ca	6	6	6	6	6	6	6	6	6	6	6	6	6
Al	0.19	0.17	0.06	0.36	1.00	0.15	0.79	0.09	0.18	0.11	0.57	0.25	0.27
Si	1.84	1.81	1.96	1.65	1.02	1.83	1.24	1.88	1.78	1.90	1.45	1.72	1.76
S^{4+}	0.04	0.16	0.40	0.43	0.51	0.62	0.71	0.80	0.92	1.09	1.24	1.32	1.54
S^{6+}	2	2	2	2	2	2	2	2	2	2	2	2	2

* Samples 1–9 are thaumasite; samples 10–13 are hielscherite; compositions are ordered by increasing S content.

** For analyses including volatiles see Table 3.

† Locality codes are: G, Graulay, Hillesheim, West Eifel; R, Rother Kopf, Gerolstein, West Eifel; S, Schellkopf, Brenk, East Eifel; Zb, Zeilberg, Franconia.

‡ The calculated SO_2 and SO_3 contents in wt.% recalculated for 2 $S^{6+}O_4$ groups per formula unit.

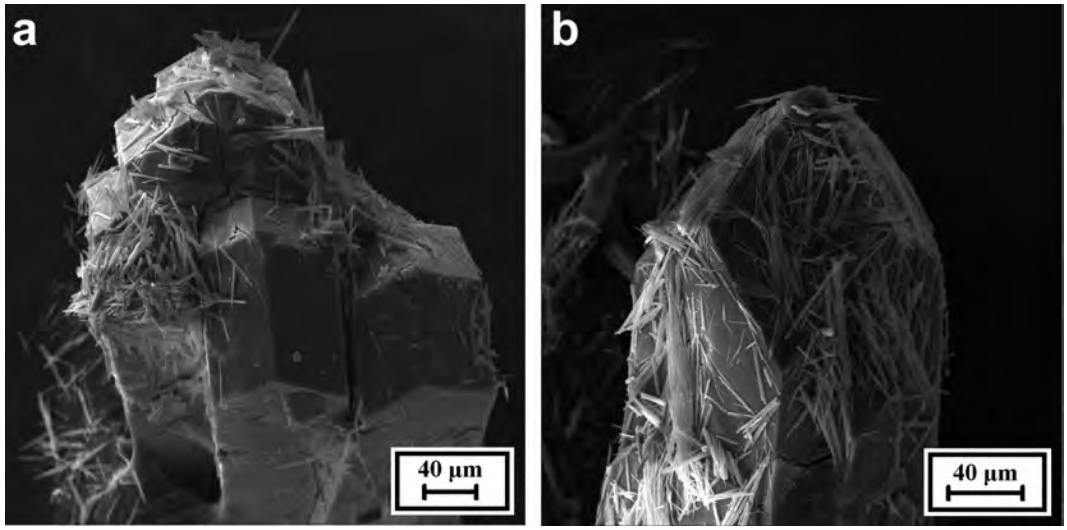

FIG. 2. Clusters of acicular hielscherite crystals on phillipsite-K on the holotype specimen (G-3049) from Graulay quarry. Secondary electron SEM image.

(e.g. sample G-3231; no. 12 in Table 2) form spectacular radiating groups (Fig. 3*c*). Unfortunately, although these crystals appear perfect, they are made up of a mosaic of smaller crystallites which prevent characterization by single-crystal X-ray diffraction techniques (see below). Associated minerals include phillipsite-K, chabazite-Ca and late gypsum.

The most sulfite-rich hielscherite that was identified (sample G-3234; no. 13 in Table 2) was the latest mineral to crystallize in fractures in basalt containing cavernous aggregates of nepheline and pyroxene with subordinate fluorapatite, magnetite and later phillipsite-K, chabazite-Ca and gismondine. It occurs also as aggregates of matted fibres up to 1 mm across in small cavities.

Sulfite-bearing thaumasite

Thaumasite in which some CO_3^{2-} is replaced by SO_3^{2-} (in the range $2 < S < 3$ a.p.f.u. for the formula with $Z = 1$; compositions 1–9 in Table 2) is much more widespread than hielscherite at Graulay and occurs in the same assemblages. The two minerals are visually indistinguishable. Sulfite-bearing thaumasite occurs as compact to open aggregates of fibrous to acicular crystals, up to 3 cm across in cavities in alkaline basalt (sample G-3225; no. 5 in Table 2), in altered xenoliths of volcanic glass (samples G-3235, G-3230 and G-3227; nos 6, 8 and 9 in Table 2), and in cavernous areas in pyroxene-nepheline (sample G-3238; no. 4 in Table 2). It also occurs as dense matted-fibrous veinlets in fractures in basalt up to 20 cm long and 0.5 cm wide (sample G-3226; no. 1 in Table 2), with earlier nepheline, pyroxene, fluorapatite and zeolites.

At the Rother Kopf basalt quarry, Gerolstein, West Eifel, sulfite-bearing thaumasite (sample R-3240; no. 2 in Table 2) occurs as fibrous spherulites up to 1 mm in diameter on phillipsite-K crystals which line cavities in alkaline basalt. At the Schellkopf quarry, Brenk, East Eifel, sulfite-rich thaumasite (sample S-3239; no. 7 in Table 2) occurs as radiating acicular spherulites up to 2 mm in diameter in fractures in a nosean-bearing phonolite with phillipsite-K, analcime, calcite and aragonite.

At the Zeilberg basalt quarry, Maroldsweisach, Franconia, Bavaria, sulfite-rich thaumasite (sample Zb-01; no. 3 in Table 2) was found by Klaus Hielscher with calcite and afwillite in cavities in alkaline basalt. It occurs as euhedral hexagonal prismatic crystals up to 0.5 mm in length and 0.1 mm in thickness.

Physical properties and optical characteristics of hielscherite

Individual hielscherite crystals are colourless and transparent with a vitreous lustre, fibrous aggregates are snow-white with a silky lustre.

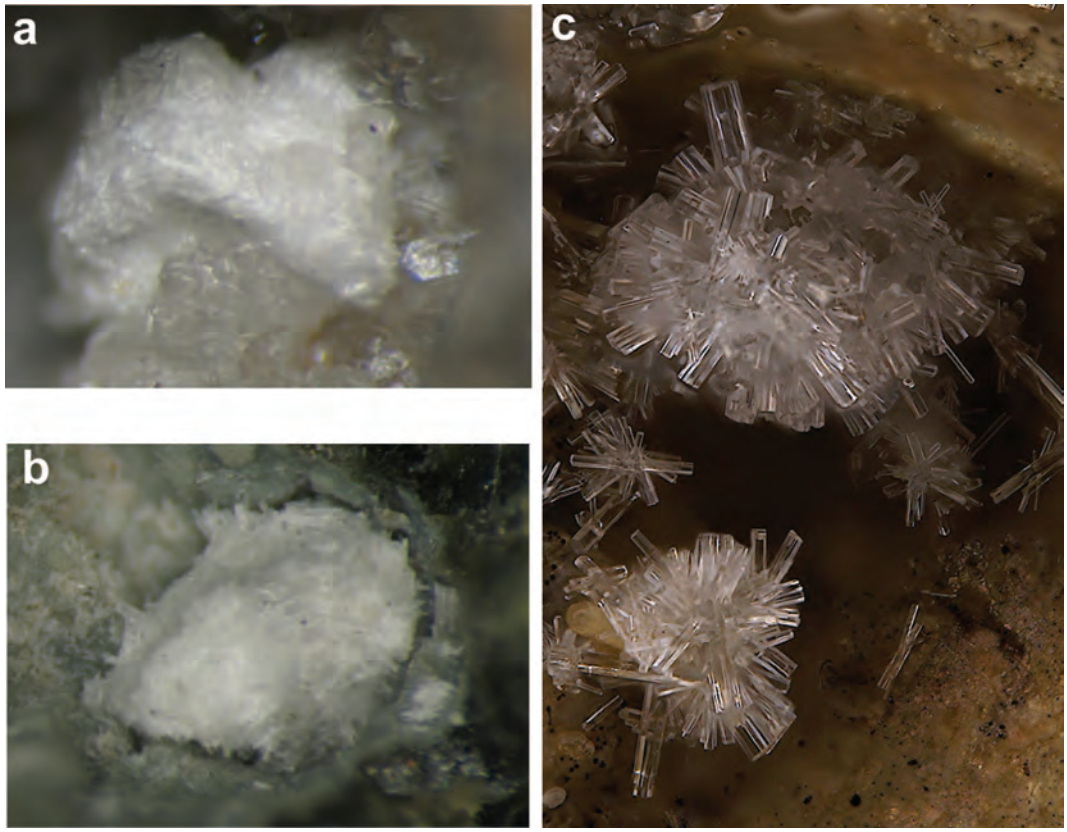

FIG. 3. Hielscherite from Graulay quarry: (*a*) matted aggregate (1 mm across) on phillipsite in a miarolitic cavity in alkaline basalt (on the holotype specimen, G-3049); (*b*) matted aggregate (1.5 mm across) filling a small gas cavity in fresh volcanic glass (G-3229); (*c*) groups of crystals (up to 0.2 mm long) in a cavity in altered volcanic glass (G-3231). Photos (*a*–*b*) I.V. Pekov and A.V. Kasatkin, (*c*) F. Krujen.

Hielscherite has a white streak. The Mohs hardness is 2–2½. Hielscherite is brittle, the cleavage is distinct on {100}, and the fracture is uneven or stepped. Sulfite-bearing varieties of thaumasite have the same properties.

The crystals on the holotype specimen of hielscherite were too small and thin for their density to be measured; the calculated density is 1.79 g cm^{-3}. For sample G-3231, the density measured by flotation in heavy liquids is 1.82(3) g cm^{-3}.

Hielscherite is uniaxial (–), with $\omega = 1.494(2)$, $\varepsilon = 1.476(2)$ in white light (data for the holotype specimen).

Infrared spectroscopy

To obtain infrared (IR) spectra (Figs. 4–6), samples were mixed with anhydrous KBr, pelletized, and analysed on a Specord 75 IR spectrophotometer at a mean resolution of 2 cm^{-1} in the range 400–1600 cm^{-1} (Figs 4 and 6) and with a Bruker ALPHA FTIR spectrometer at a resolution of 4 cm^{-1} using an average of 16 scans (Fig. 5). Polystyrene and gaseous NH_3 were used as frequency standards. In all cases the IR spectra of analogous pellets of pure KBr were used as a reference.

The IR spectra of hielscherite and sulfite-bearing thaumasite differ significantly from those of ettringite-group minerals that do not contain sulfite (Figs 4 and 5). The most characteristic feature of the sulfite-bearing members of the group is the presence of an absorption band due to SO_3^{2-} stretching vibrations at 937 cm^{-1} accompanied by weaker bands at 967 and 895 cm^{-1}. These bands are absent in the IR spectra of other ettringite-group minerals. The

presence of these bands is the best (and most easily obtained) indicator of the presence of sulfite in ettringite-group minerals.

Absorption bands in the IR spectrum of holotype hielscherite (Fig. 4, curve 4) and their assignments (using the abbreviations s = strong band, w = weak band, sh = shoulder; with all figures in cm^{-1}) are as follows: 3580(sh), 3420(s), 3100(sh) (O−H-stretching vibrations of H_2O molecules and OH groups); 1687, 1645 (bending vibrations of H_2O molecules); 1503(w), 1395 (stretching vibrations of CO_3^{2-} groups), 1107(s) (stretching vibrations of $S^{6+}O_4^{2-}$ groups); 967, 937(s), 895(w) (stretching vibrations of $S^{4+}O_3^{2-}$ groups); 740(s) (Si−O stretching vibrations in $Si(OH)_6$ octahedra); 677(s), 629(s), 572(s) (bending vibrations of SO_4^{2-} and SO_3^{2-} groups), 499(s) (O−Si−O bending vibrations in $Si(OH)_6$ octahedra). Bands due to B-bearing groups are absent.

The strongest IR-active bands produced by stretching, non-degenerate bending (A_1 mode) and degenerate bending (E mode) vibrations of the SO_3^{2-} anion are typically in the ranges 910−980, 600−660 and 430−530 cm^{-1}, respectively (Miller and Wilkins, 1952; Nakamoto, 1997; Frost and Keeffe, 2009). The strongest sulfite S−O stretching vibrations are at 917 cm^{-1} for $BaSO_3$, 943 cm^{-1} for K_2SO_3, 945 and 970 cm^{-1} for $CaSO_3{\cdot}2H_2O$, 960 cm^{-1} for Na_2SO_3 (Miller and Wilkins, 1952), and 944 and 984 cm^{-1} for hannebachite (ideally, $CaSO_3{\cdot}0.5H_2O$; Fig. 6). The presence of bands at 1492, 1430 and 861 cm^{-1} and weak bands at 1217, 1108 and 625 cm^{-1} in the IR spectrum of hannebachite from Hannebacher Lay, Eifel Mountains, is due to partial substitution of SO_3^{2-} for CO_3^{2-} and SO_4^{2-}. The IR spectrum of a synthetic sulfite analogue of ettringite with the formula $Ca_3Al(OH)_6(SO_3)_{1.5}{\cdot}13H_2O$ reported by Motzet and Pöllmann (1999) contains a strong band at 960 cm^{-1} and a weak band at 1105 cm^{-1}. The former corresponds to stretching vibrations of SO_3 groups whereas the latter can be assigned to the stretching vibrations of SO_4 groups, which are likely to have formed as a result of partial oxidation of S^{4+} to S^{6+} under atmospheric conditions.

The IR spectra of the sulfite-rich thaumasite and hielscherite are very similar (Fig. 5). The main differences are in the relative intensities of the bands corresponding to stretching vibrations of SO_3^{2-} (930−970 cm^{-1}) and CO_3^{2-} (1390−1400 cm^{-1}) anions. In the spectra of SO_3-bearing thaumasite (CO_3 > SO_3), C−O bands are significantly stronger and S^{4+}−O bands weaker than in hielscherite (SO_3 > CO_3). In the thaumasite−hielscherite solid-solution series, the intensities of the S^{4+}−O bands gradually increase and the intensities of C−O bands correspondingly decrease with increasing S (i.e. $S^{4+}O_3$) content. The relative intensities of other bands are similar in all cases (Fig. 5; Table 2).

Strong bands at 740 and 499 cm^{-1} show that $Si(OH)_6$ octahedra are present in hielscherite (Fig. 4*a*, curve 4). Similar bands are present in the IR spectra of thaumasite and kottenheimite (Fig. 4*a*, curves 2 and 1) but they are absent in the IR spectra of Si-free ettringite-group minerals, such as ettringite (Fig. 4*a*, curve 3).

The IR spectra of these minerals are also different in the 2800−3700 cm^{-1} O−H-stretching region (Figs 4*b* and 5). The most obvious differences are in the range 2900−3250 cm^{-1}, corresponding to strong hydrogen bonds. In this range, the IR spectrum of thaumasite has two or three shoulders, but the hielscherite spectrum has a single band with an absorption maximum between 3100 and 3130 cm^{-1}. The intensity of the band increases with increasing $S^{4+}O_3$ content. It is suggested that this effect is due to the polarization of H_2O molecules induced by their interaction with the S^{4+} lone-electron pair in the sulfite group (Eklund *et al*., 2012). The split H−O−H bending band in hielscherite, which has two components with maxima at 1687 and 1645 cm^{-1}, can be explained by the presence of H_2O molecules that are not equivalent symmetrically.

In contrast to kottenheimite, $Ca_3Si(OH)_6(SO_4)_2{\cdot}12H_2O$, another ettringite-group mineral with a high S content (Fig. 4*a*, curve 1), the S−O stretching vibration band in the IR spectrum of hielscherite is not split. As the distortion of SO_4 tetrahedra in kottenheimite is relatively small (S−O distances vary from 1.431 to 1.451 Å; Chukanov *et al*., 2012), we conclude that the 1088 + 1158 cm^{-1} doublet in the kottenheimite spectrum is caused by resonance interactions between adjacent sulfate groups. A weak band at 1158−1159 cm^{-1}, which is present in the IR spectra of some CO_3-deficient thaumasites, indicates partial substitution of CO_3^{2-} for SO_4^{2-}. This band is absent in the IR spectra of the samples studied in this work, which indicates that all the excess (i.e. over 1 a.p.f.u., Z = 2) sulfur is present as sulfite; this in turn allows the sulfite content to be calculated from the electron microprobe analyses. Taking this into

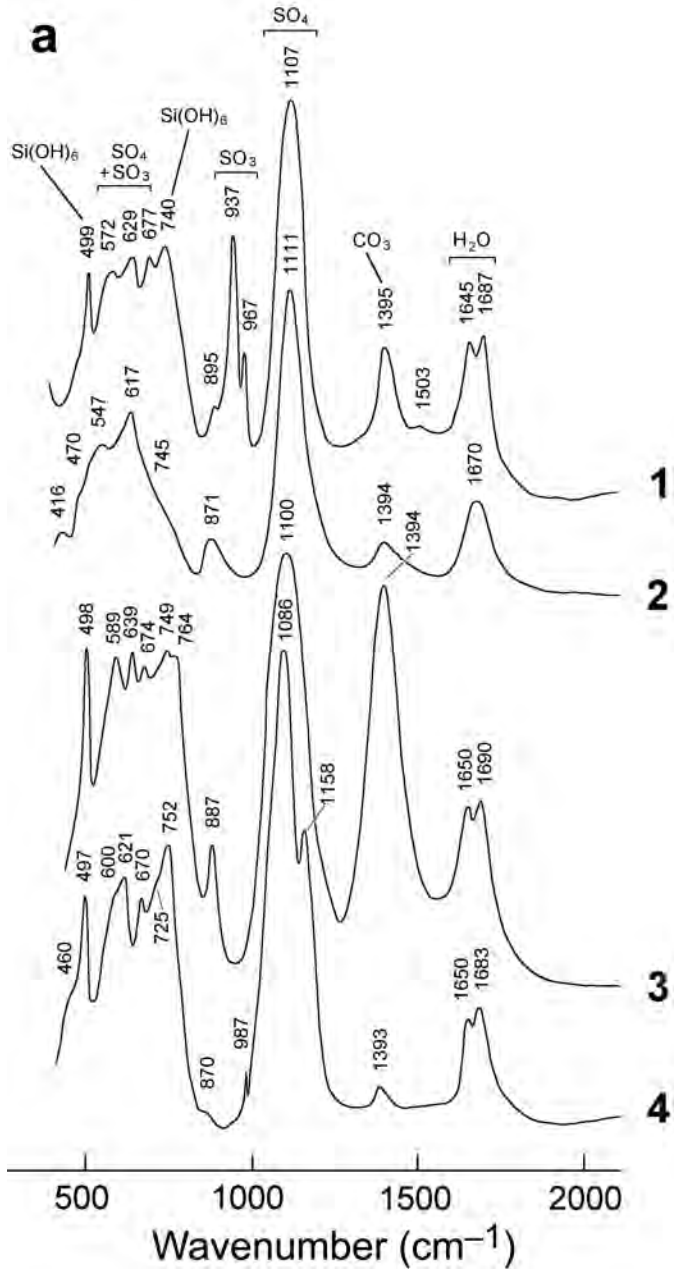

FIG. 4 (*this and facing page*). The IR spectra of (1) kottenheimite from Bellerberg, Eifel, Germany; (2) thaumasite from Uraveli, Akhaltsikhe, Georgia; (3) ettringite from Nickenicher Sattel, Eifel; and (4) holotype hielscherite G-3049 from Graulay quarry: (*a*) the region 400−2000 cm^{-1}; (*b*) the O−H-stretching region (2500−3800 cm^{-1}).

account, we conclude that the relative intensities of the bands at 937 and 967 cm^{-1} are correlated with the sulfite content (Fig. 5; Table 2).

The IR spectra of several other samples of ettringite-group minerals from late hydrothermal assemblages in the Eifel alkaline basalts (thau-

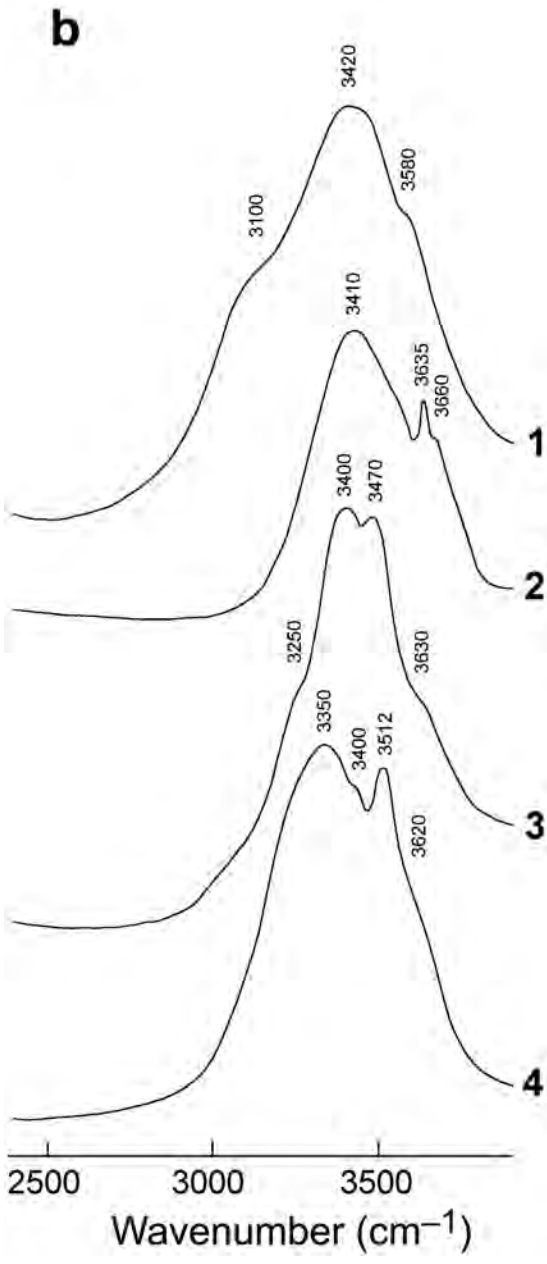

masite and ettringite from Bellerberg, Mayen, East Eifel; and ettringite and kottenheimite from Graulay) contain weak bands in the region 890–970 cm^{-1}, very close to the bands described above.

X-ray absorption near edge structure (XANES) spectroscopy

Direct determinations of the valency of sulfur in the holotype sample of hielscherite were made by XANES spectroscopy at the SUL-X beamline of the ANKA synchrotron radiation source (Institute

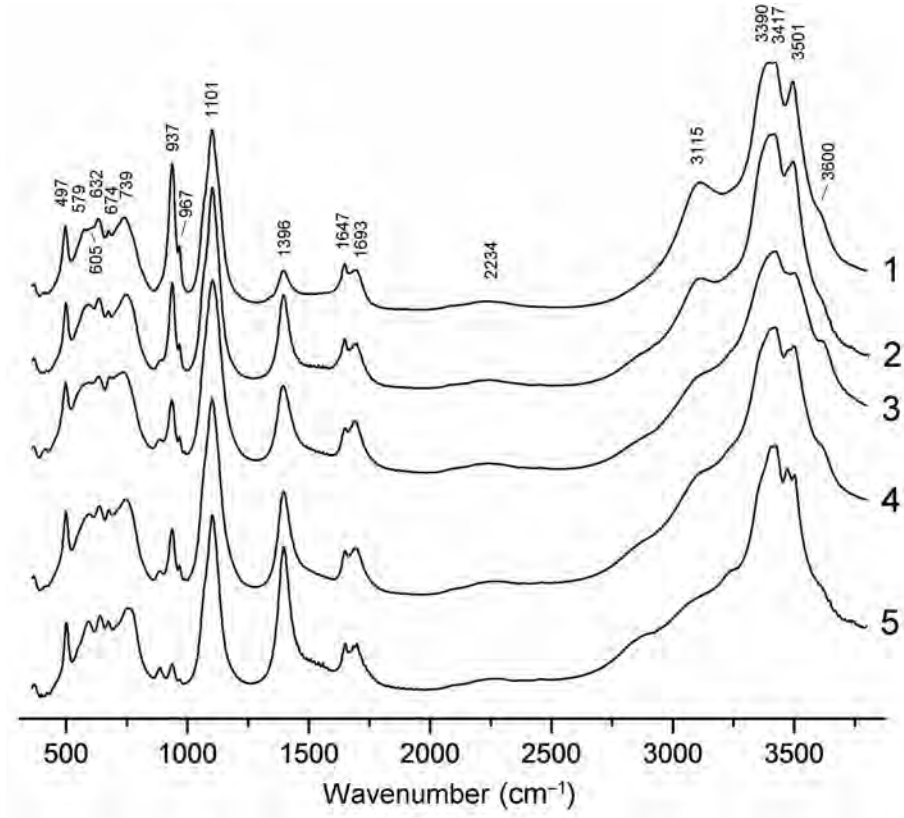

FIG. 5. The IR spectra of thaumasite–hielscherite series minerals: (1–2) hielscherite; (3–5) sulfite-bearing thaumasite. Samples are in order of decreasing SO_3 content as follows: (1) G-3234, (2) G-3231, (3) G-3227, (4) G-3235, and (5) R-3240 (for chemical data see Table 2). The IR spectrum of sample Zb-01 is almost identical to that of G-3235 (4).

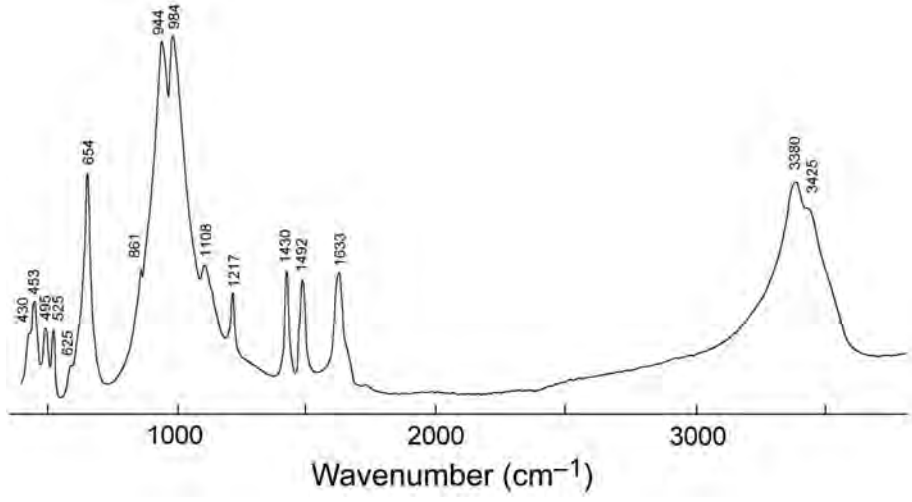

FIG. 6. The IR spectrum of hannebachite, $CaSO_3 \cdot 0.5H_2O$, from Hannebacher Lay, Hannebach, Eifel, Germany. The bands at 861, 1430, 1492 and 625, 1108, 1217 cm^{-1} correspond to admixed CO_3^{2-} and SO_4^{2-} groups.

for Synchrotron Radiation, Karlsruhe Institute of Technology, Karlsruhe, Germany). Monochromatic X-rays were generated by a Si(111) crystal pair in a double crystal monochromator, providing a fixed beam height during energy tuning. A collimated beam with a size of about 0.8×0.8 μm was chosen to minimize radiation damage. No significant changes in the spectra were observed after 10 quick scans of 3 min each. More detailed spectra were recorded from a different area on the sample for 25 min at energy step widths of 0.2 eV across the absorption edge. All measurements were performed in transmission mode using ionization chambers as detectors (Oxford IC50, modified). The hielscherite and reference spectra were pre-edge and post-edge background corrected and normalized to an edge jump of one using the *ATHENA* program from the *IFEFFIT* package (Ravel and Newville, 2005).

Figure 7 shows the S *K*-edge XANES spectrum of hielscherite compared to reference spectra of compounds with different valencies obtained with the same technique. They are characterized by two prominent absorption features, one at ~2481.4 eV, indicating S^{6+} and the other at ~2477.3 eV, indicating S^{4+}. In general the heights of these features increases with increasing valency of sulfur as seen in Fig. 7. Even the relatively low height of the feature at ~2477.3 eV in curve (*a*) indicates that a significant amount of sulfur in hielscherite is S^{4+}. The small shift in the main absorption peak between sulfite in hielscherite to sulfite in Na_2SO_3 and sulfate in hielscherite and thaumasite to sulfate in $CaSO_4$ might indicate small differences between the local chemical and electronic environment of the absorbing sulfur atom in the ettringite-type structure and in the structures of Na_2SO_3 and $CaSO_4$.

A comparison of the hielscherite spectrum with spectra of different mixtures of sulfite-free thaumasite and synthetic Na_2SO_3 showed that the sulfite/sulfate ratio in the new mineral was between 1:1 and 1:3, and closer to the 1:1 value (in agreement with structural data; see below). A check of the ratio for two different hielscherite samples showed no significant differences.

Chemical data

The Ca, Al, Si and S contents of thaumasite–hielscherite series minerals (Table 2) were determined by electron-microprobe analysis. No other elements with atomic numbers higher than oxygen were detected. The data were obtained using a Jeol JSM-6480LV scanning electron microscope equipped with an the INCA-Energy 350 energy-dispersive spectrometer. The operating voltage was 15 kV, the beam current 0.5 nA and the beam diameter 3 μm. The following standards were used: anorthite (Ca, Al, Si) and $SrSO_4$ (S). Attempts to use wavelength-dispersive spectrometry with higher beam currents were unsuccessful due to sample instability under the electron beam.

The H_2O, CO_2 and N_2O_5 content of two samples of hielscherite (G-3049 and G-3231), were determined by gas chromatography (CHN analysis) of the products of annealing at 1200ºC with a Vario Micro cubeanalyser (Elementar GmBH, Germany). Analytical data for these samples are listed in Table 3.

In Tables 2 and 3, the SO_2 and SO_3 contents are recalculated on the basis of 2.00 SO_4 per formula unit ($Z = 1$), in line with structural data (see below), which show that in hielscherite, thaumasite and minerals of the hielscherite–thaumasite solid solution series, one of the two sites in the channels (S1) is fully occupied by tetrahedrally coordinated S^{6+}, whereas the other is occupied by XO_3 anions ($X = S^{4+}$, C^{4+}, N^{5+}) and is split between trigonal pyramidal (S2: species-defining SO_3^{2-}) and triangular (C: admixture of CO_3^{2-}, NO_3^-) geometries.

The empirical formula of holotype hielscherite (G-3049) calculated on the basis of 3 Ca atoms per formula unit (a.p.f.u.) is $Ca_3(Si_{0.73}Al_{0.28})_{\Sigma 1.01}(OH)_{5.71}(SO_4)_{1.00}(SO_3)_{0.62}(CO_3)_{0.38}(NO_3)_{0.05}\cdot 10.63H_2O$. The simplified formula is $Ca_3Si(OH)_6(SO_4)(SO_3,CO_3)\cdot 11H_2O$. The ideal endmember formula, $Ca_3Si(OH)_6(SO_4)(SO_3)\cdot 11H_2O$, requires CaO 26.93, SiO_2 9.62, SO_2 10.25, SO_3 12.82, H_2O 40.38, total 100.00 wt.%.

On the basis of the compositional data (Table 2) and gradual, regular changes in the IR spectra (Fig. 5), we assume that thaumasite and hielscherite form a complete solid-solution series which extends from the common sulfite-free composition (endmember thaumasite, $Ca_3Si(OH)_6(SO_4)(CO_3)\cdot 12H_2O$) at least to a composition (sample G-3234) which contains 77 mol.% of the hielscherite endmember ($Ca_3Si(OH)_6(SO_4)(SO_3)\cdot 11H_2O$).

Table 2 also shows that minerals of the thaumasite–hielscherite series have a wide variation in their Si:Al ratio, from $Si_{1.96}Al_{0.06}$ ($Z = 1$) in sample Zb-01, to $Si_{1.02}Al_{1.00}$ in sample G-3225.

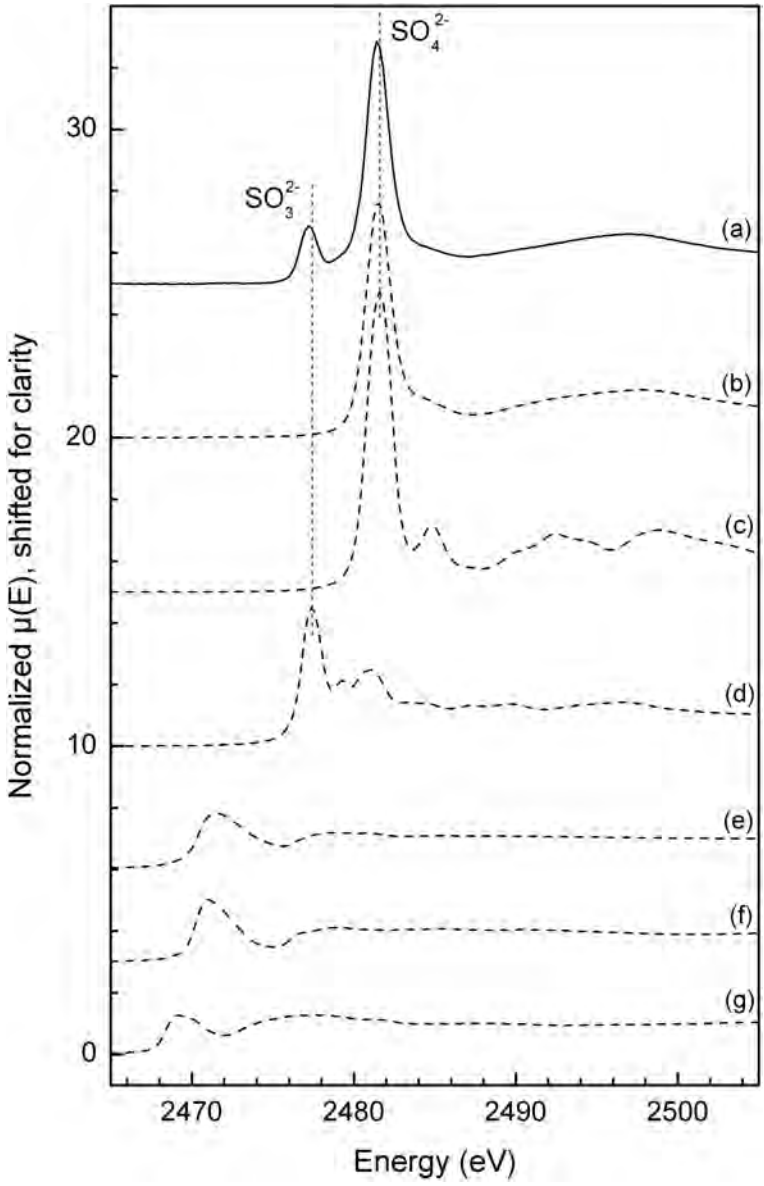

FIG. 7. The sulfur *K*-edge XANES spectrum of (a) hielscherite, with the following spectra of sulfur compounds with different S valences for comparison: (b) thaumasite; (c) synthetic $CaSO_4$ with S^{6+} in sulfate anion; (d) synthetic Na_2SO_3, with S^{4+} in the sulfite anion; (e) native sulfur, with S^o; (*f*) pyrite, FeS_2, with S_2^{2-} in disulfide; and (g) synthetic FeS with S^{2-} in sulfide.

In hielscherite, this ratio varies from $Si_{1.90}Al_{0.11}$ (G-3229) to $Si_{1.46}Al_{0.56}$ (G-3049). Significant substitution of Al for Si in the *M* octahedra is not common in thaumasite but is well documented in synthetic ettringite-type compounds. The solid-solution series between synthetic analogues of thaumasite and ettringite was studied by Barnett *et al*. (2000).

At room temperature, hielscherite slowly dissolves in HCl with very weak effervescence. Sulfite-bearing thaumasite varieties with higher CO_3^{2-} content show stronger effervescence.

TABLE 3. Chemical composition of hielscherite.

Oxide	G-3049 (holotype) Mean (wt.%) (range/SD) $n = 8$	G-3231 Mean (wt.%) (range/SD) $n = 5$
CaO	27.15 (26.5–27.9/0.3)	26.72 (26.0–27.2/0.2)
Al_2O_3	2.33 (2.0–2.6/0.2)	1.06 (0.9–1.3/0.1)
SiO_2	7.04 (6.6–7.4/0.3)	8.50 (8.1–8.8/0.2)
SO_{2calc}*	6.40	6.96
SO_{3calc}*	12.91	13.19
CO_2	2.71	2.53
N_2O_5	0.42	0.31
H_2O	39.22	40.14
Total	98.18	100.41
SO_{3meas}	20.91 (20.0–21.9/0.6)	21.89 (21.0–22.8/0.5)
Formula calculated on the basis of 6 Ca a.p.f.u. ($Z = 1$)		
Ca	6	6
Al	0.57	0.25
Si	1.45	1.72
$S^{4+}O_3$	1.24	1.32
$S^{6+}O_4$	2	2
CO_3	0.76	0.70
NO_3	0.10	0.07
OH	11.41	11.52
H_2O	21.27	21.28

* The calculated SO_2 and SO_3 contents in wt.% recalculated for 2 $S^{6+}O_4$ groups per formula unit (see text).

X-ray crystallography and crystal structure data

Of all the studied samples only Zb-01 (sulfite-bearing thaumasite) and G-3231 (hielscherite) had crystals that were suitable for single-crystal X-ray diffraction. Both of these samples were used for crystal structure analyses. The Zb-01 crystals were of sufficiently good quality to produce a reliable refinement, whereas the lower quality, highly mosaic crystals from G-3231 did not produce a good structure refinement. Apparently perfect single crystals of hielscherite (Fig. 3*c*), proved to be intergrowths of randomly oriented subparallel microdomains when examined by single-crystal X-ray diffraction. Numerous attempts to find a high-quality single crystal fragment (using STOE IPDS-II and Oxford Xcalibur S CCD diffractometers), were unsuccessful. Thus, a relatively large 'crystal' from sample G-3231 (Table 4) was used (as it produced high reflection intensities) and the results of the analysis are only considered as a structural model. The crystal structure of hielscherite (from the holotype G-3049) was refined using the Rietveld method (Schneider, 1989).

Single-crystal X-ray studies

Single-crystal X-ray studies of hielscherite (G-3231) and sulfite-rich of thaumasite (Zb-01) were carried out using a STOE IPDS II diffractometer equipped with an image plate area detector. The structures were solved by direct methods and refined using the *SHELX-97* software package (Sheldrick, 2008). Crystallographic data, data collection and structure refinement details are given in Table 4, and atom coordinates and displacement parameters in Table 5. Further details of the crystal-structure refinements have been deposited with the Principal Editors of *Mineralogical Magazine* and can be downloaded from http://www.minersoc.org/pages/e_journals/dep_mat_mm.html.

The structure of sulfite-rich thaumasite (sample Zb-01) (Fig. 8) is similar to endmember thaumasite, $Ca_3Si(SO_4)(CO_3)(OH)_6{\cdot}12H_2O$ (Edge and

TABLE 4. Crystal parameters, single-crystal data collection and structure refinement details for sulfite-bearing thaumasite (Zb-01) and hielscherite (G-3231).

Crystal Data		
Mineral	SO_3-bearing thaumasite (Zb-01)	Hielscherite (G-3231)
Crystal size (mm)	$0.35 \times 0.03 \times 0.03$	$0.75 \times 0.35 \times 0.25$
Crystal system	Hexagonal	Hexagonal
Space group	$P6_3$	$P6_3$
a (Å)	11.070(2)	11.106(2)
c (Å)	10.4397(15)	10.492(2)
V (Å^3)	1107.9(3)	1120.7(4)
Z	2	2
D (g cm^{-3})	1.91	1.86
Data Collection		
Instrument	Stoe IPDS II (image plate)	Stoe IPDS II (image plate)
Radiation	Mo$K\alpha$ (λ = 0.71073 Å)	Mo$K\alpha$ (λ = 0.71073 Å)
Average temperature (K)	293	293
Detector to sample distance (mm)	80	80
Omega increment (º)	1	2
Number of frames	180 (1 run)	180 (2 runs, 90 frames per run)
Exposure per frame (min)	4	2
2θ range (º)	4.24–50.00	4.24–55.00
Total collected reflections	6104	16,946
Unique reflections	1239	908
Unique observed $F > 4\sigma(F)$	883	834
R_{int}	0.114	0.156
hkl range	$-10 \leqslant h \leqslant 0$; $0 \leqslant k \leqslant 13$; $-12 \leqslant l \leqslant 12$	$-14 \leqslant h \leqslant 7$; $0 \leqslant k \leqslant 14$; $0 \leqslant l \leqslant 13$
Refinement		
R_1 [$F > 4\sigma(F)$]	0.045	0.099
R_1 (all data)	0.064	0.105
wR_2	0.107	0.301
S = *GooF*	0.899	2.951

Taylor, 1971; Effenberger *et al*., 1983; Martucci and Cruciani, 2006), except for the S^{4+}- and C-bearing anions. In common with endmember thaumasite, in which SO_4 and CO_3 anions are ordered (Fig. 9), the SO_3-rich mineral has SO_4 tetrahedra occupying discrete sites. The SO_4 sulfur atom (S1) is tetrahedrally coordinated by four oxygen atoms (O_{S1A} and O_{S1B}), with S–O distances of $3 \times 1.438(9)$ Å and $1 \times 1.516(1)$ Å. The site occupied by carbon atoms in thaumasite is split into two sites, C and S2 (Table 5) in sulfite-rich thaumasite. The C site is occupied by carbon (s.o.f. 50%) and the S2 site by sulfur (s.o.f. 42%). As CO_3 is in excess of SO_3 in this mineral (as also indicated by the electron microprobe and IR data) it is a sulfite-rich variety of thaumasite. The C site is coordinated by three $O_{(C,S2)}$ atoms, forming a flat triangle with C–$O_{(C,S2)}$ bond lengths of 1.342(9) Å and the S2 site forms a trigonal pyramid with three S2–$O_{(C,S2)}$ bonds of 1.497(2) Å. These configurations and interatomic distances are typical of CO_3 and $S^{4+}O_3$ anions.

The structure model obtained for hielscherite G-3231 is very similar to sulfite-rich thaumasite (Table 5). The positions of tetrahedral SO_4 groups (S1 coordinated by four oxygen ligands O_{S1A} and O_{S1B}) and pyramidal SO_3 groups (S2 and O_{S2}) were found. The C site, which has a much a smaller occupany factor, was not located in the final difference-Fourier map, probably because of the low quality of the crystal.

Powder X-ray studies and Rietveld refinement

The crystal structure of the holotype sample of hielscherite (G-3049) was refined by the Rietveld method, using the structural model obtained for sulfite-rich thaumasite (Zb-01) as a starting point.

TABLE 5. Coordinates and isotropic displacement parameters (B_{iso}, Å^2) of atoms and site occupancy factors for sulfite-bearing thaumasite (Zb-01) and hielscherite (G-3231 and G-3049).

Sample	Atom	*x/a*	*y/a*	*z/c*	B_{iso}	s.o.f.
Zb-01	Ca	0.8054(1)	0.79393(9)	0.1340(6)	1.78(2)	1
G-3231		0.8058(2)	0.7950(2)	0.1378(6)	2.07(6)	1
G-3049		0.8059(9)	0.7948(9)	0.140(5)	1.9(2)	1
Zb-01	Si	0	0	0.3880(9)	1.52(4)	1
G-3231		0	0	0.3900(11)	1.4(2)	1
G-3049		0	0	0.385(10)	1.7(7)	= $Si_{0.7}Al_{0.3}$
Zb-01	O1	0.8688(8)	0.9949(8)	0.9883(7)	1.98(2)	1
G-3231		0.877(1)	0.998(1)	0.9943(11)	2.0(2)	1
G-3049		0.869(4)	0.995(7)	0.9878(16)	1.8(9)	1
Zb-01	O2	0.0072(9)	0.8758(8)	0.2791(7)	1.58(2)	1
G-3231		0.0116(12)	0.8735(16)	0.2867(15)	2.8(2)	1
G-3049		0.007(5)	0.876(3)	0.2796(16)	1.5(8)	1
Zb-01	O3	0.6644(11)	0.658(1)	0.9545(10)	3.95(2)	1
G-3231		0.6710(15)	0.6638(15)	0.9581(16)	2.8(3)	1
G-3049		0.664(4)	0.659(3)	0.955(2)	4.0(9)	1
Zb-01	O4	0.7705(4)	0.6085(4)	0.632(1)	3.32(1)	1
G-3231		0.7710(12)	0.6093(11)	0.640(2)	4.0(2)	1
G-3049		0.771(3)	0.609(2)	0.631(8)	3.5(9)	1
Zb-01	O5	0.8582(4)	0.5967(4)	0.138(1)	2.84(1)	1
G-3231		0.8574(11)	0.5983(10)	0.1417(18)	3.3(2)	1
G-3049		0.858(2)	0.5969(19)	0.140(8)	3.0(9)	1
Zb-01	O6	0.6722(7)	0.6529(8)	0.3148(9)	2.13(2)	1
G-3231		0.6695(14)	0.6497(18)	0.317(2)	4.0(4)	1
G-3049		0.672(3)	0.653(3)	0.315(2)	2.2(8)	1
Zb-01	S1 = S^{6+}	⅓	⅔	0.3764(7)	2.45(2)	0.85(3)
G-3231		⅓	⅔	0.3742(8)	2.3(2)	1
G-3049		⅓	⅔	0.375(4)	2.5(8)	0.98
Zb-01	O_{S1A}	⅓	⅔	0.2312(9)	2.84(3)	1
G-3231		⅓	⅔	0.237(2)	4.0(5)	1
G-3049		⅓	⅔	0.231(4)	3(1)	1
Zb-01	O_{S1B}	0.4259(9)	0.6199(9)	0.4216(11)	2.13(3)	1
G-3231		0.4307(19)	0.6228(14)	0.421(2)	4.5(4)	1
G-3049		0.426(4)	0.620(4)	0.421(3)	2(1)	1
Zb-01	C	⅓	⅔	0.85(2)	1.6(2)	0.5(2)
G-3231		–	–	–	–	–
G-3049		⅓	⅔	0.85(3)	2(1)	0.39
Zb-01	S2 = S^{4+}	⅓	⅔	0.911(3)	0.32(5)	0.42(7)
G-3231		⅓	⅔	0.8956(16)	4.5(2)	1
G-3049		⅓	⅔	0.914(5)	1(1)	0.59
Zb-01	$O_{(C,S2)}$	0.370(1)	0.8020(9)	0.8473(8)	3.71(2)	1
G-3231		0.372(2)	0.8042(18)	0.8503(15)	3.9(3)	1
G-3049		0.370(4)	0.802(2)	0.849(3)	4(1)	1

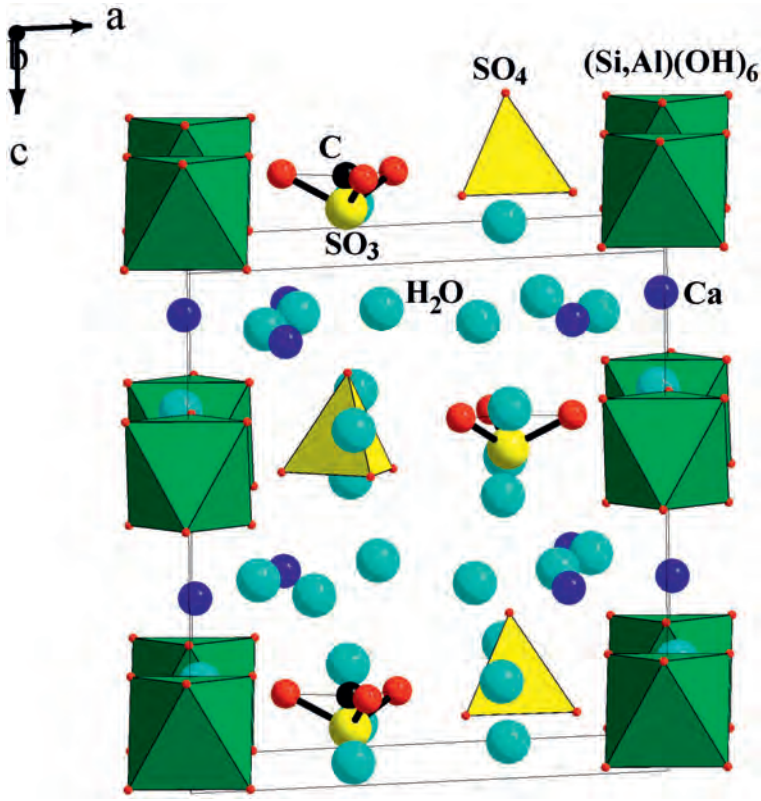

FIG. 8. Crystal structures of hielscherite and sulfite-rich thaumasite. They differ primarily in the occupancies of the S2 sites (corresponding to SO_3 groups) and the C sites (see text). The unit cell is shown.

Data were collected using a STOE–STADI MP powder diffractometer (Cu$K\alpha_1$ radiation, λ = 1.54056 Å). The range 7.0 ⩽ 2θ ⩽ 81.68º was measured at a step width of 0.02º. Data treatment and Rietveld structure analysis were carried out using the *Wyriet* computer program package (Schneider, 1989). The profiles were modelled using pseudo-Voigt functions. Final agreement indices are R_p = 0.0236, R_{wp} = 0.0317, R_{Bragg} = 0.0227 and R_F = 0.0283. The mineral is hexagonal, space group $P6_3$, with a = 11.1178(2), c = 10.5381(2) Å and V = 1128.06(4) Å^3.

The crystal structure of holotype hielscherite is very similar to that of sulfite-rich thaumasite sample Zb-01 (Table 5; Figs 8 and 9). The main differences are in the occupancy factors of the C and S2 sites, which are 39% and 59%, respectively. The dominance of SO_3 over CO_3 at this site, as indicated by the electron microprobe and IR data, was confirmed by crystal-structure refinement. The S1 site is tetrahedrally coordinated [S–O distances are 3 × 1.456(2) Å and 1 × 1.517(2) Å] and is occupied by S^{6+}. The SO_3 and CO_3 groups are in a similar configuration to sulfite-rich thaumasite: triangular CO_3^{2-} and trigonal pyramidal SO_3^{2-} anions have a common base consisting of three $O_{(C,S2)}$ atoms, and the C and S2 sites are 0.66 Å apart. The C–$O_{(C,S2)}$ and S2–$O_{(C,S2)}$ bond lengths are 1.35(1) and is 1.516(2) Å, respectively.

The observed and calculated X-ray powder diffraction patterns for holotype hielscherite are in very good agreement (Table 6).

Discussion

Sulfite-bearing ettringite-group minerals, including the new mineral hielscherite in which sulfite is a species-defining anion, are relatively common late-stage phases in young alkaline volcanic rocks in southwest Germany.

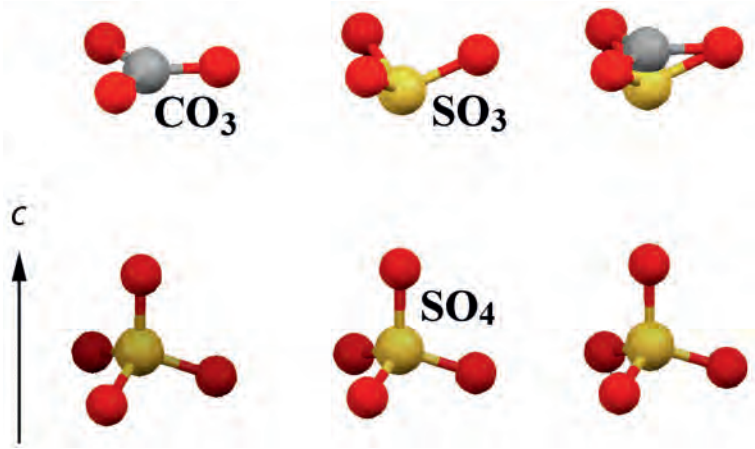

FIG. 9. The arrangement of CO_3, SO_3 and SO_4 anions in the crystal structures of thaumasite–hielscherite series minerals: (left) sulfate and carbonate groups in thaumasite (Effenberger *et al*., 1983); (right) sulfate and superimposed sulfite/carbonate groups in hielscherite and SO_3-bearing thaumasite; (middle) presumed arrangement of sulfate and sulfite groups in the hypothetical CO_3-free hielscherite endmember $Ca_3Si(SO_4)(SO_3)(OH)_6{\cdot}11H_2O$.

Compounds with an ettringite-type structure have a considerable affinity for the sulfite anion. The sulfite analogue of ettringite is well-known as a synthetic phase (Pöllmann *et al*., 1989; Motzet and Pöllmann, 1999; Grier *et al*., 2002). We believe that systematic studies of ettringite-group minerals from different localities, using IR spectroscopy as a method of detection, will reveal more sulfite-bearing compositions.

In hielscherite and sulfite-rich thaumasite, pyramidal sulfite groups occupy the same structural sites as triangular carbonate groups, and the triangular arrangement of the O atoms is similar. Tetrahedral sulfate groups are located in a separate sites. This shows that sulfate and sulfite anions in ettringite-group minerals have an ordered distribution, and there is a good reason for the subdivision of the S data obtained from the electron-microprobe analysis into S^{6+} and S^{4+} (see above). The proposed arrangement of SO_4 and SO_3 groups in a hypothetical hielscherite structure with a sulfate:sulfite ratio of 1:1 is shown in Fig. 9.

Hielscherite, ideally $Ca_3Si(OH)_6(SO_4)(SO_3){\cdot}11H_2O$, is a sulfite analogue of thaumasite, $Ca_3Si(OH)_6(SO_4)(CO_3){\cdot}12H_2O$, and buryatite, $Ca_3Si(OH,O)_6(SO_4)[B(OH)_4]{\cdot}12H_2O$ (Table 1). Although these minerals have slightly different H_2O contents, variable H_2O contents are well known in ettringite-group minerals. Indeed, Martucci and Cruciani (2006) showed that thaumasite structures with 9 to 15 H_2O molecules p.f.u. (Z = 2) are stable, and Skoblinskaya *et al*., (1975) reached a similar conclusion for ettringite. The increase in H_2O content produces a change in the Ca coordination environment; trigonal $Ca(OH)_4(H_2O)_2$ prisms are transformed into polyhedra with higher numbers of H_2O vertices as the water content increases. Significant structural transformations in the ettringite-type structure occur only if the number of H_2O molecules is reduced to less than 9 p.f.u. (Skoblinskaya *et al*., 1975). The value measured for hielscherite (from gas chromatography data) is close to 10.6 H_2O molecules p.f.u., which is in the stable range for ettringite-type structures.

Other sulfite-bearing minerals have been reported in low-temperature hydrothermal assemblages in the alkaline basalts of the Eifel volcanic region. The most common of these is hannebachite, $CaSO_3{\cdot}0.5H_2O$, which occurs at several localities in the region, including Graulay (Hentschel *et al*., 1985; Hentschel, 1993). Orschallite, $Ca_3(SO_4)(SO_3)_2{\cdot}12H_2O$, another mineral which contains ordered sulfate and sulfite anions, was first discovered at Hannebacher Lay in the West Eifel, in a similar assemblage (Weidenthaler *et al*., 1993). This study shows that ettringite-group minerals can serve as a reservoir for sulfite in geological settings similar to those in the Eifel. The presence of these minerals should be viewed as a geochemical indicator of moderately oxidizing conditions in low-temperature hydrothermal systems.

TABLE 6. X-ray powder diffraction data for holotype hielscherite (G-3049).

I_{meas} (%)	d_{meas} (Å)	I_{calc} (%)	d_{calc} (Å)	*hkl*
100	9.62	100	9.6145	010, 100
50	5.551	50	5.5543	110
10	4.910	10	4.9132	111
5	4.796	6	4.8107	020, 200
37	4.616	37	4.6189	012, 102
2	4.373	3	4.3760	021, 201
64	3.823	65	3.8219	112
4	3.635	4	3.6372	120
16	3.551	16	3.5522	022, 202
25	3.436	25	3.4381	121, 211
2	3.342	2	3.2983	013, 103
15	3.204	15	3.2079	030, 300
2	3.091	1	3.0688	031, 301
7	2.973	6	2.9682	113
1	2.778	1	2.7783	220
38	2.742	38	2.7399	032, 302
3	2.669	3	2.6694	130, 310
12	2.638	12	2.6335	004
11	2.587	12	2.5876	131, 311
37	2.528	37	2.5264	123, 213
2	2.453	2	2.4575	222
6	2.380	5, 1	2.3811, 2.3798	132, 312; 114
5	2.311	4	2.3103	024, 204
7	2.207	7	2.2082	230, 320
35	2.180	4, 32	2.1887, 2.1790	042, 402; 223
7	2.165	8	2.1612	231, 321
17	2.125	17	2.1252	133, 313
3	2.097	3	2.1005	140, 410
1	2.060	1	2.0599	141, 411
1	2.058	1	2.0582	015, 105
6	2.037	5	2.0363	232, 322
3	1.971	2	1.9701	115
3	1.950	3	1.9511	142, 412
7	1.925	7	1.9252	050, 500
10	1.825	6, 4	1.8245, 1.8233	331; 125, 215
6	1.791	2, 1, 3	1.8082, 1.8027, 1.7926	052, 502; 143, 413; 241, 421
7	1.752	2, 5	1.7559, 1.7476	006; 332
5	1.730	1, 4	1.7289, 1.7274	150, 510; 016, 106
3	1.678	3	1.6743	116
6	1.652	4, 3	1.6540, 1.6427	135, 315; 152, 512
8	1.644	8	1.6423	144, 414
5	1.604	5	1.6044	060, 600
1	1.580	1	1.5826	340, 430
8	1.556	2, 6	1.5650, 1.5543	341, 431; 054, 504
5	1.487	3, 2	1.4844, 1.4794	226; 252, 522

Another ettringite-group mineral which has recently been described from the Eifel district is kottenheimite, $Ca_3Si(OH)_6(SO_4)_2{\cdot}12H_2O$, the most sulfate-rich member of the ettringite group. All of the anion positions in its structure are occupied by SO_4 groups [the formula is $...(SO_4)_{1.97}(CO_3)_{0.09}$]. Although it was first discovered at Bellerberg quarry (Chukanov *et al*., 2012), kottenheimite also occurs at Graulay, in similar assemblages to minerals of the thaumasite–hielscherite series. It occurs as white spherulitic aggregates up to 1.5 mm in diameter, made up of hair-like crystals, overgrowing phillipsite-K in cavities in an altered xenolith of volcanic glass in alkaline basalt. It is possible that this mineral is a product of the alteration of hielscherite by post-crystallization oxidation of S^{4+} to S^{6+}. Rapid oxidation of sulfite to sulfate by atmospheric oxygen was reported by Motzet and Pöllmann (1999) in a synthetic analogue of ettringite.

Conclusions

The data collected on sulfite-rich members of the ettringite group in this work suggests the following conclusions:

(1) Ettringite-group minerals have a distinct affinity for sulfite. In their crystal structures, pyramidal sulfite groups occupy the same position as triangular carbonate groups, with analogous sites for the O atoms, whereas tetrahedral sulfate groups occupy separate positions. The sulfite–sulfate arrangement is therefore ordered.

(2) Thaumasite and the new mineral species hielscherite form a continuous solid-solution series which ranges in natural material from sulfite-free thaumasite, $Ca_3Si(OH)_6(SO_4)(CO_3){\cdot}12H_2O$, to a composition with at least 77 mol.% of endmember hielscherite, $Ca_3Si(OH)_6(SO_4)(SO_3){\cdot}11H_2O$. In this series, the SO_3:CO_3 ratio is variable, whereas the SO_4 content remains constant.

(3) Sulfite-bearing ettringite-group minerals, including hielscherite, in which sulfite is a species-defining anion, are relatively common hydrothermal minerals in young alkaline volcanic rocks in southwest Germany, especially the alkaline basalts of the Eifel region.

(4) Infrared spectroscopy is a very effective tool in the characterization of sulfite-bearing ettringite-group minerals. Infrared spectra allow reliable and routine semi-quantitative determinations of the SO_3, SO_4, and CO_3 anions, the

presence of the $Si(OH)_6$ groups and the character of the SO_4 distribution ('kottenheimite splitting'). The method is sensitive to sulfite content; even small amounts of sulfite are clearly visible in a routine IR absorption spectra on powdered samples.

Acknowledgements

We are grateful to Klaus Hielscher and Günter Blass for the providing us with some of the samples for this study, to Marina F. Vigasina for her assistance in the IR measurements and to Herbert Pöllmann, Natalia V. Zubkova and Ralph Steininger for fruitful discussions. We also thank Peter Leverett, Herta Effenberger, an anonymous referee and the Associate Editor Stuart Mills for comments on the manuscript. We acknowledge ANKA for providing beamtime for the project (reference Inh-SULX-008-110126). Single-crystal X-ray diffraction studies were carried out in the SPbSU X-ray Diffraction Resource Centre. This work was supported by the Russian Foundation for Basic Research, grant numbers 11-05-00397-a and 11-05-00407-a.

References

Anthony, J.W., Bideaux, R.A., Bladh, K.W. and Nichols M.C. (1995) *Handbook of Mineralogy. Vol. II. Silica, Silicates*. Mineral Data Publishing, Tucson, Arizona, USA.

Barnett, S.J., Adam, C.D. and Jackson, A.R.W. (2000) Solid solutions between ettringite and thaumasite. *Journal of Materials Science*, **35**, 4109–4114.

Basso, R., Lucchetti, G. and Palenzona, A. (1991) Gravegliaite, $MnSO_3{\cdot}3H_2O$, a new mineral from Val Graveglia (Northern Apennines, Italy). *Zeitschrift für Kristallographie*, **197**, 97–106.

Batic, O.R., Milanesi, C.A., Maiza, P.J. and Marfil, S.A. (2000) Secondary ettringite formation in concrete subjected to different curing conditions. *Cement and Concrete Research*, **30**, 1407–1412.

Brown, P.W. and Hooton, R.D. (2002) Ettringite and thaumasite formation in laboratory concretes prepared using sulfate-resisting cements. *Cement and Concrete Composites*, **24**, 361–370.

Brown, P.W., Hooton, R.D. and Clark, B.A. (2003) The co-existence of thaumasite and ettringite in concrete exposed to magnesium sulfate at room temperature and the influence of blast-furnace slag substitution on sulfate resistance. *Cement and Concrete Composites*, **25**, 939–945.

Chukanov, N.V., Britvin, S.N., Van, K.V., Möckel, S. and Zadov, A.E. (2012) Kottenheimite, $Ca_3Si(OH)_6(SO_4)_2{\cdot}12H_2O$, a new ettringite-group mineral from the Eifel area, Germany. *The Canadian Mineralogist*, **50**, 55–63.

Dunn, P.J., Peacor, D.R., Leavens, P.B. and Baum, J.L. (1983) Charlesite, a new mineral of the ettringite group, from Franklin, New Jersey. *American Mineralogist*, **68**, 1033–1037.

Edge, A. and Taylor, H.F.W. (1971) Crystal structure of thaumasite $[Ca_3Si(OH)_6{\cdot}12H_2O](SO_4)(CO_3)$. *Acta Crystallographica*, **B27**, 594–601.

Effenberger, H., Kirfel, A., Will, G. and Zobetz, E. (1983) A further refinement of the crystal structure of thaumasite, $Ca_3Si(OH)_6(SO_4)\ (CO_3){\cdot}12H_2O$. *Neues Jahrbuch für Mineralogie, Monatshefte*, **1983**, 60–68.

Eklund, L., Hofer, T.S., Pribil, A.B., Rode, B.M. and Persson, I. (2012) On the structure and dynamics of the hydrated sulfite ion in aqueous solution – an *ab initio* QMCF MD simulation and large angle X-ray scattering study. *Journal of the Chemical Society, Dalton Transactions*, **41**, 5209–5216.

Frost, R.L. and Keeffe, E.C. (2009) Raman spectroscopic study of the sulfite-bearing minerals scotlandite, hannebachite and orschallite: implications for the desulfation of soils. *Journal of Raman Spectroscopy*, **40**, 244–248.

Granger, M.M. and Protas, J. (1969) Détermination et étude de la structure cristalline de la jouravskite $Ca_3Mn^{IV}(SO_4)(CO_3)(OH)_6{\cdot}12H_2O$. *Acta Crystallographica*, **B25**, 1943–1951.

Grier, D.G., Jarabek, E.L., Peterson, R.B., Mergen, L.E. and McCarthy, G.J. (2002) Rietveld structure refinement of carbonate and sulfite ettringite. *Advances in X-ray Analysis*, **45**, 194–199.

Gross, S. (1980) Bentorite. A new mineral from the Hatrurim Area, west of the Dead Sea, Israel. *Israel Journal of Earth Sciences*, **29**, 81–84.

Hentschel, G. (1993) Die Lavaströme der Graulai: eine neue Fundstelle in der Westeifel. *Lapis*, **18**(9), 11–23.

Hentschel G., Tillmanns, E. and Hofmeister, W. (1985) Hannebachite, natural calciumsulfate hemihydrate, $CaSO_3{\cdot}1/2H_2O$. *Neues Jahrbuch für Mineralogie, Monatschefte*, **1985**, 241–250.

Jacobsen, S.D., Smyth, J.R. and Swope, R.J. (2003) Thermal expansion of hydrated six-coordinate silicon in thaumasite, $Ca_3Si(OH)_6(CO_3)(SO_4){\cdot}12H_2O$. *Physics and Chemistry of Minerals*, **30**, 321–329.

Malinko, S.V., Chukanov, N.V., Dubinchuk, V.T., Zadov A.E. and Koporulina, E.V. (2001) Buryatite, $Ca_3(Si,Fe^{3+},Al)[SO_4](OH)_5O{\cdot}12H_2O$, a new mineral. *Zapiski Vserossiyskogo Mineralogicheskogo Obshchestva*, **130**, 72–78, [in Russian].

Martucci, A. and Cruciani, G. (2006) *In situ* time resolved synchrotron powder diffraction study of

thaumasite. *Physics and Chemistry of Minerals*, **33**, 723–731.

McDonald, A.M., Petersen, O.V., Gault, R.A., Johnsen, O., Niedermayr, G., Brandstätter, F. and Giester, G. (2001) Micheelsenite, $(Ca,Y)_3Al(PO_3OH,CO_3)(CO_3)(OH)_6{\cdot}12H_2O$, a new mineral from Mont Saint-Hilaire, Quebec, Canada and the Nanna pegmatite, Narsaarsuup Qaava, South Greenland. *Neues Jahrbuch für Mineralogie, Monatschefte*, **2001**, 337–351.

Merlino, S. and Orlandi, P. (2001) Carraraite and zaccagnaite, two new minerals from the Carrara marble quarries: their chemical compositions, physical properties, and structural features. *American Mineralogist*, **86**, 1293–1301.

Miller, F.A. and Wilkins, C.H. (1952) Infrared spectra and characteristic frequencies of inorganic ions. *Analytical Chemistry*, **24**, 1253–1294.

Moore, A.E. and Taylor, H.F.W. (1970) Crystal structure of ettringite. *Acta Crystallographica*, **B26**, 386–393.

Motzet, H. and Pöllmann, H. (1999) Synthesis and characterisation of sulfite-containing AFm phases in the system $CaO–Al_2O_3–SO_2–H_2O$. *Cement and Concrete Research*, **29**, 1005–1011.

Nakamoto, K. (1997) *Infrared Spectra of Inorganic and Coordination Compounds*. *Part A*. Fifth edition. John Wiley and Sons, New York.

Paar, W.H., Braithwaite, R.S.W., Chen, T.T. and Keller, P. (1984) A new mineral, scotlandite ($PbSO_3$) from Leadhills, Scotland: the first naturally occurring sulphite. *Mineralogical Magazine*, **48**, 283–288.

Pöllmann, H., Kuzel, H.-J. and Wenda, R. (1989) Compounds with ettringite structure. *Neues Jahrbuch für Mineralogie, Abhandlungen*, **160**, 133–158.

Pushcharovsky, D.Yu., Lebedeva, Yu.S., Zubkova, N.V., Pasero, M., Bellezza, M., Merlino S. and Chukanov N.V. (2004) The crystal structure of sturmanite. *The Canadian Mineralogist*, **42**, 723–729.

Ravel, B. and Newville, M. (2005) *ATHENA*, *ARTEMIS*, *HEPHAESTUS*: data analysis for X-ray absorption spectroscopy using *IFEFFIT*. *Journal of Synchrotron Radiation*, **12**, 537–541.

Schneider, J. (1989) *Profile refinement on IBM-PCs*. International Workshop on the Rietveld Method, Petten, The Netherlands.

Sheldrick, G.M. (2008) A short history of *SHELX*. *Acta Crystallographica*, **A64**, 112–122.

Skoblinskaya, N.N., Krasilnikov, K.G., Nikitina, L.V. and Varlamov, V.P. (1975) Changes in crystal structure of ettringite on dehydration. 2. *Cement and Concrete Research*, **5**, 419–431.

Weidenthaler, C., Tillmanns, E. and Hentschel, G. (1993) Orschallite, $Ca_3(SO_3)_2SO_4{\cdot}12H_2O$, a new calcium-sulfite-sulfate-hydrate mineral. *Mineralogy and Petrology*, **48**, 167–177.

Weiss, S. (1990) *Mineralfundstellen, Deutschland West*. Weise, Munich, Germany.